Supporting Information

Seuront and Stanley 10.1073/pnas.1322363111

SI Text

Study Species, Sampling, and Acclimation. *Temora longicornis* is very abundant in coastal temperate waters of the Northern Hemisphere (1). It represents from 35% to 70% of the total population of copepods in the Southern Bight of the North Sea (2, 3) and is able to remove up to 49% of the daily primary production (4). Its naupliar stages significantly contribute to larval fish diet (5). *Eurytemora affinis* is one of the most abundant zooplankton species in the brackish part of Northern Hemisphere estuaries, usually localized around the Maximum Turbidity Zone (6), and plays a significant role in estuarine food webs as an important food supply for many fishes, shrimps, and mysids (7).

T. longicornis were collected with a WP2 (200-μm mesh size) from the inshore surface waters of the Eastern English Channel (50°40′75″N, 1°31′1″E) at a temperature of 18 °C and a salinity of 32 practical salinity unit (PSU). *E. affinis* individuals were collected from the Seine estuary using a WP2 net (200-μm mesh size) at a temperature of 19 °C in the low salinity zone (S = 4 PSU) at low tide near the Pont de Tancarville (49°28′26″N, 0°27′47″W). Sampling occurred in late August for *T. longicornis* and early September for *E. affinis*. For both species, specimens were gently diluted in 30-L isotherm tanks using, respectively, in situ seawater and estuarine water and transported to the laboratory where adult males and females were immediately sorted by pipette under a dissecting microscope. *T. longicornis* were reared in 20-L aquaria filled with filtered (Whatman GF/C glass-fiber filters, porosity 0.45 μm) in situ coastal seawater to which was added a suspension of *Rhodomonas salina* and *Isochrisis galbana* (1:1) at a concentration of 5×10^6 cells/L (8). The larger heterotrophic fagellate *Oxyrrhis marina* was present as an additional food source (9). *E. affinis* adults were reared in 20-L aquaria filled with filtered (Whatman GF/C glass-fiber filters, porosity 0.45 μm) in situ estuarine water to which was added a suspension of *R. marina* and *I. galbana* (2/3:1/3) at a concentration of $\sim 10^7$ cells/L, a mixture promoting proper development and reproduction of *E. affinis* in culture (10, 11). *T. longicornis* and *E. affinis* were reared under constant conditions of temperature (18 °C) and salinity (32 and 4 PSU, respectively) under a 12/12-h light/dark cycle.

Selection of Virgin Males and Females. Immediately after field collection, adult *T. longicornis* females ($n = 50$) and *E. affinis* ovigerous females ($n = 50$) were sorted under a binocular microscope and transferred into 60-mL beakers equipped with 200-μm mesh chambers filled with 50 mL of filtered seawater (GF/C Whatman, 0.45-μm porosity). The inner chamber was used for separating eggs and females to prevent the predation of females on eggs. Beakers were inspected every 12 h by removing the inner chamber. Eggs were counted using a binocular microscope and transferred into aerated 1-L beakers filled with culture solution for incubation. The development of naupliar and copepodite stages was monitored every 24 h. Males and females were separated when reaching the copepodite 5 stage and kept separated in 20-L aquaria filled with culture solution under constant conditions of temperature (18 °C) and salinity (32 and 4 PSU for *T. longicornis* and *E. affinis*, respectively) under a 12/12-h light/dark cycle. The behavioral experiments took place within 24 h after males and females reached the copepodite 6 stage.

Choice of the Scaling Range Used to Estimate the Function $\zeta(q)$. The moments of order $q(q > 0)$ of the norm of 3D displacements $\|\Delta X_\tau\|$ depend on the temporal increment τ as

$$\left\langle \|\Delta X_\tau\|^q \right\rangle \sim \tau^{\zeta(q)}. \quad \text{[S1]}$$

The exponents $\zeta(q)$ were estimated as the slope of the linear trend of $\langle \|\Delta X_\tau\|^q \rangle$ vs. τ in log-log plots (Fig. S2). However, because an objective criterion is needed to decide on the appropriate range of scales to include in the regressions, we used the values of τ that satisfied two optimization criteria. First, we consider a regression window of varying width that ranges from a minimum of five data points to the entire data set. The smallest windows are slid along the entire data set at the smallest available increments, with the entire procedure iterated $(n - 4)$ times, where n is the total number of available data points. Within each window and for each width, we estimate the coefficient of determination (r^2) and the sum of the squared residuals for the regression. We subsequently use the values of τ (Eq. **1**) that maximize the coefficient of determination and minimize the total sum of the squared residuals to define the scaling range and to estimate the related exponents, $\zeta(q)$. Second, noting that Eq. **S1** is equivalent to

$$d \log\left[\left\langle \|\Delta X_\tau\|^q \right\rangle\right] \Big/ d \log \tau = \zeta(q). \quad \text{[S2]}$$

it appears that a scaling regime will manifest itself as a slope of 0 in plots of $d \log\left[\left\langle \|\Delta X_\tau\|^q \right\rangle\right] / d \log \tau$ vs. $\log \tau$. The range of scales exhibiting a nil slope was estimated using the abovementioned procedure, and the significance of the differences between the slope of each regression and the expected slope line of 0 was directly tested using standard statistical analysis (12). The scaling range was then defined as the scales that statistically satisfied both optimization criteria. Also note that the intercept of the range of scales exhibiting a zero-slope behavior provides the exponents $\zeta(q)$.

Moment Function $\zeta(q)$ as an Objective Tool to Assess the Quantitative Nature of Searching Patterns. The moment function $\zeta(q)$ estimated from Eq. **1** following the procedure described previously can be unambiguously used to identify a model of searching from empirical behavioral data. Specifically, for Brownian motion, $\zeta(q) = q/2$; hence, whenever $\zeta(2) = 1$, the process corresponds to normal diffusion. In contrast, anomalous diffusive processes are characterized by $\zeta(2) \neq 1$ (13). Using only the second-order moment $q = 2$ to infer the presence of normal diffusion can, however, be misleading as some processes have $\zeta(2) = 1$ and hence are apparently diffusing normally, whereas for other moments (14), $\zeta(q) \neq q/2$. This approach is generalized to fractional Brownian motion, defined as $\zeta(q) = qH$, where $H = \zeta(1)$, with the limits $\zeta(q) = 0$ and $\zeta(q) = q$ corresponding, respectively, to confinement and localization, and ballistic motion; anomalous diffusion commonly occurs when $H \neq 1/2$ (15). Superdiffusion corresponds to the case where the mean squared displacement grows superlinearly in time ($H > 1/2$) and subdiffusion leads to sublinear scaling in time ($H < 1/2$) (15). The mean and the variance are not sufficient to quantify the behavior of probability density functions. A complete description requires an infinite number of moments; hence, we used the whole function $\zeta(q)$ instead of a single exponent (16, 17). For finite-length Lévy flights (i.e., truncated Lévy flights), the function $\zeta(q)$ is bilinear with $\zeta(q) = q/(\mu - 1)$ for $q < \mu - 1$ and $\zeta(q) = 1$ for $q \geq \mu - 1$ (18, 19); the exponent μ $(1 < \mu \leq 3)$ characterizes the power-law tail of the probability distribution of the move-step length l as $P(l) \sim l^{-\mu}$, where $1 < \mu \leq 3$. For $\mu \geq 3$, the mean and the variance of the

move-step lengths are both finite; as a consequence of the central-limit theorem, their distribution is Gaussian. For $1 < \mu < 3$, the scaling is superdiffusive (i.e., the search pattern is tailored to minimize the distance traveled while locating prey), whereas the value $\mu = 2$ indicates that the scaling becomes quadratic in time and corresponds to the lower extreme of superdiffusive processes that is a Lévy flight. The turnover in scaling above $q = \mu - 1$ is, however, spurious in the sense that it does not reflect the exponent μ of the infinite length time series (20). For constant-velocity Lévy walks, $\zeta(2) = 2$ for $\mu < 2$ (21) and more generally $\zeta(q) = q$ for $\mu < 2$, whereas $\zeta(2) = 4 - \mu$ for $2 < \mu < 3$ (21). Note, however, that although no general expression for the function $\zeta(q)$ has been proposed yet, in the long time limit, the behavior of constant-velocity Lévy walks converges toward the behavior of Lévy flights (22). However, the intermittent velocities of both *T. longicornis* and *E. affinis*, ranging from very likely slow steps to rare and extremely rapid displacements (Fig. S1), are incompatible with a constant-velocity Lévy walk. The velocity needs not to be a constant (21), in which case the behavior of the function $\zeta(q)$ has yet to be defined. Finally, when the function $\zeta(q)$ is nonlinear and convex, the resulting diffusion is referred to as being multifractal (17, 23), hence the term multifractal anomalous diffusion or multifractal random walk (17, 24). The significance of the differences between the empirical values of the function $\zeta(q)$ and their theoretical expectations for ballistic and Brownian motion, $\zeta(q) = q$ and $\zeta(q) = q/2$, was inferred using a modified t test (12).

Behavioral Experiments. To determine whether *T. longicornis* and *E. affinis* would react to background pheromone concentration, both males and females were exposed to control water and to male- and female-conditioned water. Control water was prepared from in situ coastal and estuarine water filtered (Whatman GF/C glass-fiber filters, porosity 0.45 μm) and subsequently autoclaved. Control water was transferred in sterile plastic vials and frozen until the behavioral experiments took place. To create pheromone-conditioned water, *T. longicornis* males and females and *E. affinis* males, nonovigerous females, and ovigerous females were placed separately in beakers containing control water at a density of 1, 5, 10, 20, 50, and 100 animals per liter, respectively, to test for cue intensity. Males and females were allowed to condition the water for 24 h. After incubation was completed, female-conditioned and male-conditioned water was transferred to sterile plastic vials and frozen until the behavioral experiments took place.

Behavioral experiments were conducted in a cubic (15 × 15 × 15 cm) glass chamber in a temperature-controlled (18 °C) room and in the dark and at night to avoid any potential behavioral artifact related to the diel cycle of the copepods (25). Before each experiment, 10 adult individual (male or female for *T. longicornis* and male, nonovigerous female, or ovigerous female for *E. affinis*) was transferred in the experimental filming setup filled up with control water, male-conditioned water, or female-conditioned water and were allowed to acclimatize for 15 min (25). Individuals were only used once. For each treatment, behavioral experiments were replicated 10 times, and the treatments (control seawater, male-conditioned, and female-conditioned water) were randomized. The experimental chamber was rinsed with acetone and distilled water and allowed to dry between trials to remove any chemical scent. The size of *T. longicornis* adult males (0.98 ± 0.01 mm; mean ± SD) and females (1.15 ± 0.01 mm) and *E. affinis* adult males (0.86 ± 0.01 mm), adult nonovigerous females (0.89 ± 0.01 mm), and ovigerous females (0.90 ± 0.02 mm) used in the experiments did not significantly differ between treatments and replicates (Kruskal-Wallis test, $P > 0.05$).

3D trajectories of freely swimming *T. longicornis* adult males and females and *E. affinis* males, nonovigerous females, and ovigerous females were recorded at a rate of 25 frame/s using two synchronized and orthogonally oriented infrared digital cameras (DV Sony DCR-PC120E) facing the experimental chamber. Six arrays of 72 infrared-light-emitting diodes (LEDs) provided the only light source from the bottom of the chamber. The cameras overlooked the experimental chamber from the side and hence represented the *x-z* and *y-z* planes of the experimental chamber, and the various components of the set-up were adjusted so that the copepods were adequately resolved and in focus. 3D swimming paths were obtained by combining information from the 2D views. Each experiment lasted 60 min, after which valid video clips were selected for analysis. Valid video clips consisted of pathways in which the organisms were swimming freely, at least two body lengths away from any chamber's walls or seawater surface (25, 26). To ensure the statistical relevance of the present work, paths of the same duration (i.e., $d = 120$ s) were selected, and the same number ($n = 50$) of swimming paths was considered. Based on our sampling rate of 25 frame/s, each replicate experiment was then based on the analysis of $25 \times 120 \times 50 = 150{,}000$ successive positions, resulting in 1,500,000 data points (10 replicates) for each control and each of the six behavioral experiments conducted on *T. longicornis* (virgin males and females, males and females) and *E. affinis* (virgin males and females, males and females, and ovigerous females). These experiments resulted in 42,000,000 data points for *T. longicornis* and 52,500,000 data points for *E. affinis*. Selected video clips were captured (DVgate Plus) as MPEG movies and converted into QuickTime movies (QuickTime Pro), after which the x, y, and z coordinates of swimming pathways were automatically extracted and combined into a 3D picture using LabTrack software (DiMedia). The time step was always 0.04 s, and output sequences of (x_t, y_t, z_t) coordinates were subsequently used to characterize the motion behavior.

First-Order vs. Second-Order Multifractal Phase Transitions. Multifractal phase transitions occur when the structure function exponents $\zeta(q)$ defined from the scaling properties of the fluctuations of the norm $||\Delta X_\tau||$ of copepod 3D displacements (Eq. **1**) lose their nonlinearity and become linear after a critical order of moment q_c. More specifically, multifractal phase transitions relate to the occurrence of a maximum intermittency value $\gamma_{\max}$ and refer to either first- or second-order multifractal phase transition. For first-order multifractal phase transition, $\gamma_{\max}$ is the maximum value taken by a given variable associated with the occurrence of very rare and violent intermittencies. In contrast, for a second-order multifractal phase transition, $\gamma_{\max}$ corresponds to the maximum intermittency effectively detected from a finite sample size. In both cases, for statistical moments q verifying $q \geq q_c$, the function $\zeta(q)$ follows a linear asymptotic behavior related to $\gamma_{\max}$ as (17)

$$\zeta(q) = 1 - \gamma_{\max} q. \quad \textbf{[S3]}$$

In the case of sampling limitations, the critical exponent q_s is given as

$$q_s \propto D_s, \quad \textbf{[S4]}$$

where D_s is the sampling dimension defined as

$$D_s = 1 + \log N_s / \log \lambda, \quad \textbf{[S5]}$$

where N_s is the number of independent realizations, and λ is the ratio between the largest and the smallest scales over which the norm $||\Delta X_\tau||$ of copepod 3D displacements exhibits a scaling behavior defined as $\langle ||\Delta X_\tau||^q \rangle \propto \tau^{\zeta(q)}$. From Eqs. **S3–S5**, it is shown that q_s increases with the number of independent realiza-

tions. First- and second-order multifractal phase transitions then respectively occur when $q_c < q_s$ and $q_c \geq q_s$.

When seawater was conditioned with more than 10 females, the functions $\zeta(q)$ estimated from the search patterns of *T. longicornis* adult males become linear after a critical moment of order q_c that is decreasing as $q_c = 5.2$, $q_c = 4.1$, and $q_c = 3.0$ for seawater, respectively, conditioned with 20 (Fig. S4*A*), 50 (Fig. S4*B*), and 100 females (Fig. S4*C*). The critical moments of order q_c are related to a first-order multifractal phase transition as their values were independent of the sample size and were consistently significantly smaller than the critical exponent q_s ($P < 0.05$). As a consequence, the critical moments q_c are associated with the occurrence of extremely rare large displacements (17). Although this does not bring anything to the search pattern issue *sensu stricto*, it nevertheless shows (*i*) that the shape of the function $\zeta(q)$ is not related to sampling limitations and (*ii*) biologically indicates that *T. longicornis* males exhibit very large relocation jumps under condition of high pheromone concentrations that are increasingly more violent with the intensity of the chemical cue used to condition the water. The similarity between those jumps and the violent escape reactions of copepods in response to a range of stressors (27) led us to suggest that this behavior might be related to an escape behavior under stressful conditions of hyperstimulation of their sensory system.

Heterospecific Pheromone Recognition in *T. longicornis* and *E. affinis*. To determine whether *T. longicornis* and *E. affinis* would react to heterospecific background pheromone concentration, both virgin and adult males and females were exposed to water conditioned with the pheromones of males and females of the other species. To create heterospecific pheromone-conditioned water, *T. longicornis* males and females and *E. affinis* males, nonovigerous females, and ovigerous females were placed separately in beakers containing control water at a density of 1, 5, 10, 20, 50, and 100 animals per liter, respectively, to test for cue intensity. Males and females were allowed to condition the water for 24 h. After incubation was completed, female-conditioned and male-conditioned water was transferred to sterile plastic vials and frozen until the behavioral experiments took place. Before each experiment, 10 experimental individuals (*T. longicornis* or *E. affinis*) were transferred in the experimental filming setup filled up with water conditioned with the other species and were allowed to acclimatize for 15 min (28, 29). All experimental individuals were used only once. Behavioral experiments were replicated five times and randomized. The function $\zeta(q)$ obtained for *T. longicornis* adult and virgin males and females under the condition of water conditioned with *E. affinis* did not significantly differ from the function $\zeta(q)$ obtained under control conditions (Wilcoxon–Mann–Whitney U test, $P > 0.05$). Similarly, the function $\zeta(q)$ obtained for *E. affinis* adult and virgin males and females and ovigerous females under the condition of water conditioned with *T. longiornis* did not significantly differ from the function $\zeta(q)$ obtained under control conditions (Wilcoxon–Mann–Whitney U test, $P > 0.05$). These results are consistent with a reproductive isolation of *T. longicornis* and *E. affinis*.

Heterospecific Mating Behavior in *T. longicornis* and *E. affinis*. The existence of heterospecific behaviors were assessed in no-choice mating experiments, with all specimens of each sex belonging to one species only. Heterospecific experiments were consistently conducted with five specimens of each species according to the following five treatments: *T. longicornis* males × *E. affinis* nonovigerous females, *T. longicornis* males × *E. affinis* ovigerous females, *T. longicornis* males × *E. affinis* males, *T. longicornis* females × *E. affinis* nonovigerous females, and *T. longicornis* females × *E. affinis* ovigerous females. Before each experiment, the 10 experimental individuals were transferred in the experimental filming setup filled up with control water and were allowed to acclimatize for 15 min (28, 29). All experimental individuals were used only once. Heterospecific experiments were replicated five times and randomized. None of the swimming paths observed exhibit any sign of trail following behavior toward heterospecific individuals of the same and opposite sex, suggesting a reproductive isolation of *T. longicornis* and *E. affinis*.

1. Razouls C, de Bovée F, Kouwenberg J, Desreumaux N (2005–2010) Diversity and geographic distribution of marine planktonic copepods. Available at http://copepodes.obs-banyuls.fr/en. Accessed January 11, 2014.
2. Daan R (1989) Factors controlling the summer development of the copepod populations in the Southern Bight of the North Sea. *Neth J Sea Res* 23(3):305–322.
3. Seuront L (2005) First record of the calanoid copepod *Acartia omorii* (Copepoda: Calanoide: Acartiidae) in the southern bight of the North Sea. *J Plankton Res* 27(12): 1301–1306.
4. Dam HG, Peterson WT (1993) Seasonal contrasts in the diel vertical distribution, feeding behaviour and grazing impact of the copepod *Temora longicornis*. *J Mar Res* 51(3):561–594.
5. Ringuette M, Castonguay M, Runge JA, Gregoire F (2002) Atlantic mackerel (*Scomber scombrus*) recruitment fluctuations in relation to copepod production and juvenile growth. *Can J Fish Aquat Sci* 59(4):646–656.
6. Soetaert K, Van Rijswijk P (1993) Spatial and temporal patterns of the zooplankton in the Westerchelde estuary. *Mar Ecol Prog Ser* 97:47–59.
7. Fockedey N, Mees J (1999) Feeding of the hyperbenthic mysid *Neomysis integer* in the maximum turbidity zone of the Elbe, Westerschelde and Gironde estuaries. *J Mar Syst* 22(2-3):207–228.
8. Klein Breteler WCM (1980) Continuous breeding of marine pelagic copepods in the presence of heterotrophic dinoflagellates. *Mar Ecol Prog Ser* 2:229–233.
9. van Duren L, Videler JJ (1995) Swimming behaviour of development stages of the calanoid copepod *Temora longicornis* at different food concentrations. *Mar Ecol Prog Ser* 126:153–161.
10. Lavens P, Sorgeloos P (1996) *Manual on the Production and Use of Live Food for Aquaculture. FAO Fisheries Technical Paper* (FAO, Rome), Vol 361.
11. Devreker D, Souissi S, Winkler G, Forget-Leray J, Leboulanger F (2009) Effects of salinity, temperature and individual variability on the reproduction of *Eurytemora affinis* (Copepoda; Calanoida) from the Seine estuary: A laboratory study. *J Exp Mar Biol Ecol* 368(2):113–123.
12. Zar J (1996) *Biostatistical Analysis* (Prentice Hall, Englewood Cliffs, NJ).
13. Metzler R, Klafter J (2000) The random walk's guide to anomalous diffusion: A fractional dynamics approach. *Phys Rep* 339(1):1–77.
14. Ferrari R, Manfroi AJ, Yong WR (2001) Strongly and weakly self-similar diffusion. *Physica D* 154(1-2):111–137.
15. Sokolov IM (2001) Lévy flights from a continuous-time process. *Phys Rev E Stat Nonlin Soft Matter Phys* 63(1 Pt 1):011104.
16. Bacry E, Delour J, Muzy JF (2001) Multifractal random walk. *Phys Rev E Stat Nonlin Soft Matter Phys* 64(2 Pt 2):026103.
17. Seuront L (2010) *Fractals and Multifractals in Ecology and Aquatic Science* (CRC Press, Boca Raton, FL).
18. Chechkin AV, Gonchar VYu (2000) Self and spurious multi-affinity of ordinary Lévy motion, and pseudo-Gaussian relation. *Chaos Solitons Fractals* 11(14):2379–2390.
19. Nakao H (2000) Multi-scaling properties of truncated Lévy flights. *Phys Lett A* 266(4-6):282–289.
20. Chapman SC, Hnat B, Rowlands G, Watkins NW (2005) Scaling collapse and structure functions: Identifying self-affinity in finite length time series. *Nonlinear Process Geophys* 12(6):767–774.
21. Klafter J, Shlesinger MF, Zumofen G (1996) Beyond Brownian motion. *Phys Today* 49(2):33–39.
22. Metzler R (2000) Generalized chapman-kolmogorov equation: A unifying approach to the description of anomalous transport in external fields. *Phys Rev E Stat Phys Plasmas Fluids Relat Interdiscip Topics* 62(5 Pt A):6233–6245.
23. Seuront L, Schmitt F, Lagadeuc Y, Schertzer D, Lovejoy S (1999) Multifractal analysis as a tool to characterize multiscale inhomogeneous patterns. Example of phytoplankton distribution in turbulent coastal waters. *J Plankton Res* 21(5):877–922.
24. Schmitt F, Seuront L (2001) Multifractal random walk in copepod behavior. *Physica A* 301(1-4):375–396.
25. Seuront L (2011) Behavioral fractality in marine copepods: Endogenous rhythms vs. exogenous stressors. *Physica A* 309(2):250–256.
26. Seuront L (2013) Chemical and hydromechanical components of mate-seeking behaviour in the calanoid copepod *Eurytemora affinis*. *J Plankton Res* 28(4):724–743.
27. Buskey EJ, Lenz PH, Hartline DK (2002) Escape behavior of planktonic copepods in response to hydrodynamic disturbances: High speed video analysis. *Mar Ecol Prog Ser* 235:135–146.
28. Seuront L (2006) Effect of salinity on the swimming behaviour of the estuarine calanoid copepod *Eurytemora affinis*. *J Plankton Res* 28(9):805–813.
29. Seuront L (2010) Zooplankton avoidance behaviour as a response to point sources of hydrocarbon contaminated water. *Mar Freshw Res* 61(3):263–270.

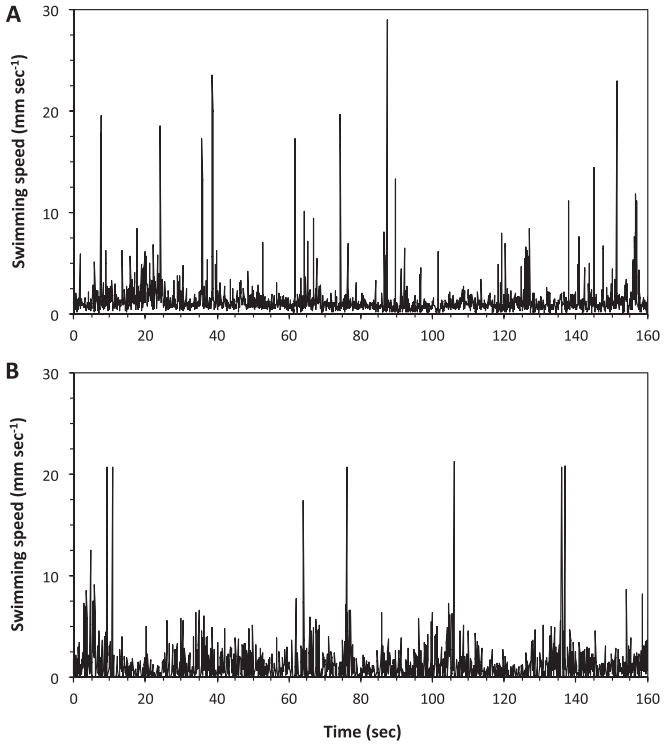

Fig. S1. Illustration of the intermittent fluctuations perceptible from the occurrence of very long and rare moves over a wide range of shorter, more frequent moves in time series of *T. longicornis* (*A*) and *E. affinis* (*B*) successive displacements.

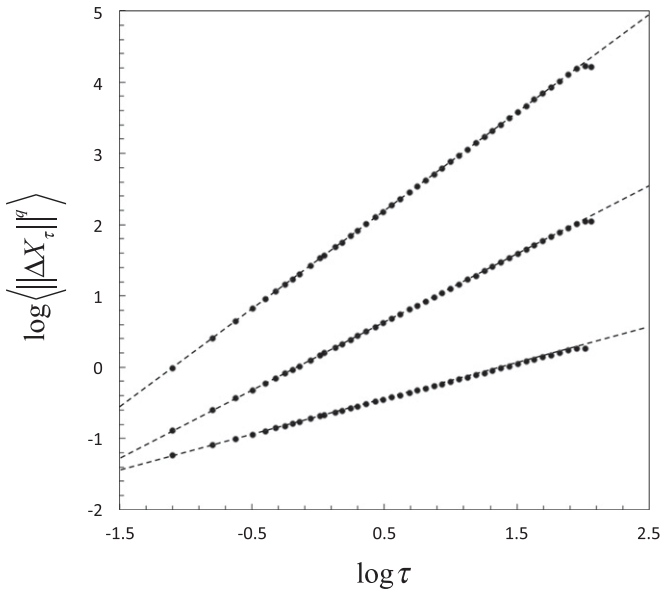

Fig. S2. Log-log plot of the structure functions $\langle \|\Delta X_\tau\|^q \rangle$ characterizing the displacements, ΔX_τ of adult males *E. affinis* swimming freely in estuarine water conditioned with 20 nonovigerous females as a function of a time increment τ. The dashed lines are the best linear fits of Eq. **1** following the optimization criteria described above, for statistical moments $q = 1$, $q = 2$, and $q = 3$ from bottom to top. The scaling regime ranges from time increments bounded between 0.08 and nearly 90 s; hence, the nondimensional scale ratio is approximately $\lambda = 1{,}000$. No significant differences were found in the values of λ estimated for *T. longicornis* and *E. affinis* under different water treatments (Kruskal-Wallis test, $P > 0.05$).

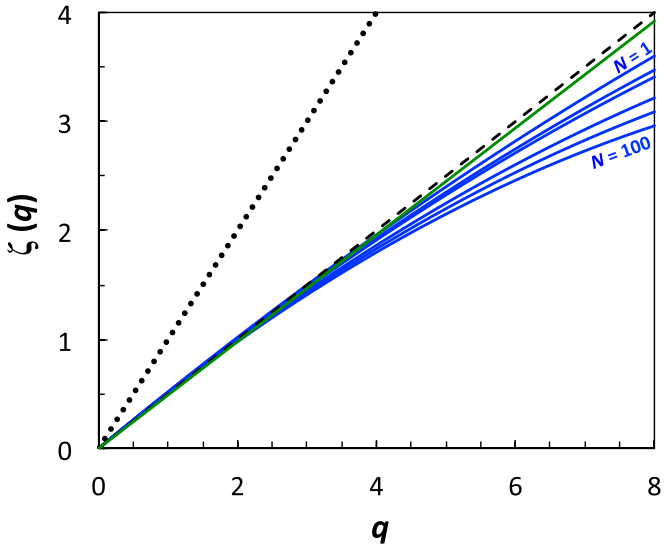

Fig. S3. Effects of water conditioning on the search strategy of *E. affinis* males. Male diffusive properties are shown under conditions of increasing cue concentration from ovigerous females obtained using control water that, respectively, held $n = 1$, 5, 10, 20, 50, and 100 ovigerous females per liter during 24 h. The diffusive properties of virgin males are shown in green. The nonlinearity of the function $\zeta(q)$ shows the multifractal anomalous diffusive nature of *E. affinis* motion behavior. The linear functions expected for ballistic motion [$\zeta(q) = q$; dotted line] and Brownian motion [$\zeta(q) = q/2$; dashed line] are shown for comparison.

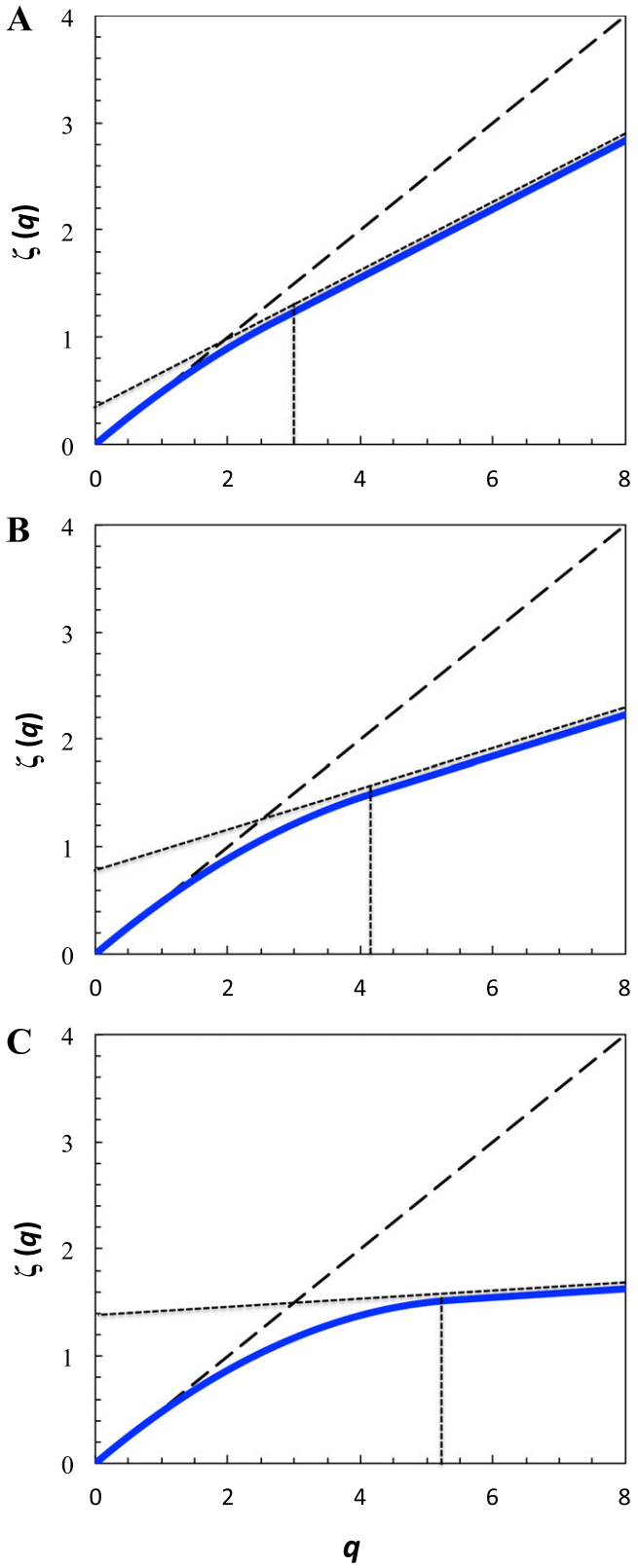

Fig. S4. Illustration of the estimation of the critical moment of order q_c from the empirical function $\zeta(q)$ obtained from the search patterns of *T. longicornis* adult males (blue). The linear asymptotic behavior of the function $\zeta(q)$ (dotted lines) leads to estimate the critical moment of order as $q_c = 3.0$, $q_c = 4.1$, and $q_c = 5.2$ for seawater, respectively, conditioned with 100 (*A*), 50 (*B*), and 20 females (*C*). The dashed line correspond to the theoretical function $\zeta(q)$ of a Brownian motion, i.e., $\zeta(q) = q/2$. The vertical dotted lines indicate the critical moment of order q_c.

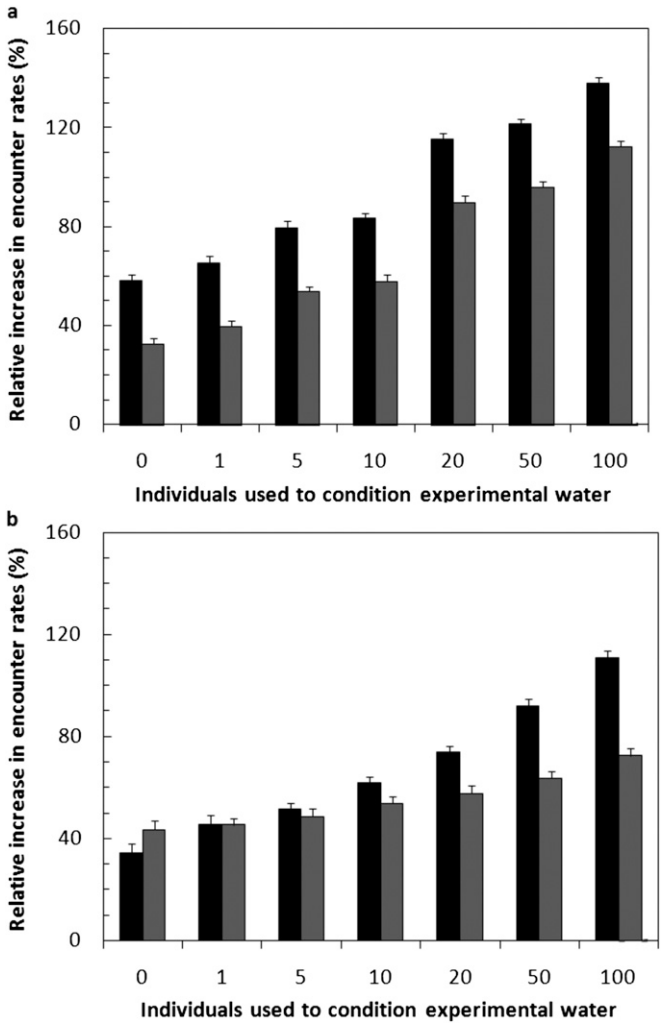

Fig. S5. Relative increase in male-female encounter rates between random walkers and multifractal random walkers as a function of the number of individuals used to conditioned experimental water for *T. longicornis* (*A*) and *E. affinis* (*B*). Encounter rates between males and virgin females are shown in gray and between both *T. longicornis* males and females and *E. affinis* males and nonovigerous females in black. The error bars are the SDs of the encounter rates averaged over the 10 replicate experiments conducted under each experimental condition.

Table S1. Synthesis of the search patterns observed for the calanoid copepods *T. longicornis* and *E. affinis* in the absence of chemical cues (control water) and in water conditioned with conspecific of the opposite sex

	Control water			Conditioned water			
Species/sex	Diffusion	Model	Fractal/ multifractal	Diffusion	Model	Fractal/ multifractal	Density dependence
T. longicornis							
Male	Superdiffusive	Ballistic/MFRW*	Fractal/multifractal*	Superdiffusive/ subdiffusive	MFRW	Multifractal	Yes
Virgin male	Normal	Bm	Fractal	Normal	Bm	Fractal	No
Female	Superdiffusive	Ballistic/MFRW*	Fractal/multifractal*	Subdiffusive	MFRW	Multifractal	No
Virgin female	Superdiffusive	Ballistic/MFRW*	Fractal/multifractal*	Superdiffusive	Ballistic/MFRW*	Fractal/multifractal*	No
E. affinis							
Male†	Superdiffusive	Ballistic/MFRW*	Fractal/multifractal*	Subdiffusive	MFRW	Multifractal	Yes
Virgin male†	Normal	Bm	Fractal	Normal	Bm	Fractal	No
Female	Superdiffusive	Ballistic/MFRW*	Fractal/multifractal*	Subdiffusive	MFRW	Multifractal	Yes
Virgin female	Superdiffusive	Ballistic/MFRW*	Fractal/multifractal*	Superdiffusive	Ballistic/MFRW*	Fractal/multifractal*	No
Ovigerous female	Superdiffusive	fBm	Fractal	Superdiffusive	fBm	Fractal	No

Bm, Brownian motion; fBm, fractional Brownian motion; MFRW, multifractal random walk.

*The observed search patterns did not significantly diverge from a ballistic (fractal) motion for low statistical moments and from a multifractal random walk for high statistical moments.

†The same search patterns were observed for males and virgin males swimming in water conditioned by nonovigerous and ovigerous females.